Electronic Supplementary Material (ESI) for Nanoscale.

ELECTRONIC SUPPLEMENTARY INFORMATION

Impact of Size and Shape Distributions on the Electron Charge Transfer Properties of Silver Nanoparticles

B. Sun* and A. S. Barnard

Molecular & Materials Modelling, DATA61 CSIRO, Door 34 Goods Shed, Village St, Docklands VIC, Australia 3008, Australia

E-mail: Baichuan.Sun@data61.csiro.au

Comparison Between DFTB and DFT

To confirm the reliable accuracy of SCC-DFTB for the Ag nanoparticles considered, we performed a comparison with the Density Function Theory (DFT). In this case we have used DFT within the Generalized Gradient Approximation (GGA) the exchange–correlation functional Perdew-Burke-Ernzerhof (PBE),[1] with the Projector Augmented Wave (PAW) potentials.[2,3] This has been implemented via the Vienna Ab initio Simulation Package (VASP)[4,5] which utilizes an iterative self–consistent scheme to solve the Kohn–Sham equations using an optimized charge-density mixing routine. Each model structure was fully relaxed, prior to the calculation of the total energies. The electronic relaxation technique used herein is an efficient matrix–diagonalization routine based on a sequential band–by–band residual minimization method of single–electron energies,[6,7] with direct inversion in the iterative subspace; whereas the ionic relaxation involves minimization of the Hellmann–Feynman forces. The initial relaxations and the following static single point energy calculations were performed with a plane–wave basis up to 312 eV, and an energy convergence of 10^{-4} eV, including full spin polarization. The geometry parameters of selected Ag nanoparticles from DFTB and DFT are given in Tab. 1 and 2, and their geometry similarity is illustrated in Fig. 1.

Table 1: Geometry properties of Ag nanoparticles from DFTB computations.

ID	Geometry	Atom Number	Mean Bond Length	Bond Length Error	Mean Bond Angle	Bond Angle Error	Diameter nm	Aspect Ratio	Formation Energy	Fermi Energy
Ag75-DH	DH	75	2.89	0.16	93.36	33.74	1.13	1.24	0.47	-3.68
Ag101-DH	DH	101	2.90	0.14	94.07	34.00	1.27	1.33	0.41	-3.61
Ag146-DH	DH	146	2.92	0.13	94.72	34.55	1.49	1.39	0.35	-3.75
Ag147-IH	IH	147	2.93	0.13	94.55	34.21	1.48	1.20	0.33	-3.75

Table 2: Geometry properties of Ag nanoparticles from DFT computations.

ID	Geometry	Atom Number	Mean Bond Length	Bond Length Error	Mean Bond Angle	Bond Angle Error	Diameter nm	Aspect Ratio	Formation Energy	Fermi Energy
Ag75-DH	DH	75	2.91	0.06	93.36	33.71	1.14	1.27	0.44	-3.41
Ag101-DH	DH	101	2.91	0.04	94.09	34.03	1.30	1.40	0.39	-3.03
Ag146-DH	DH	146	2.92	0.05	94.76	34.62	1.48	1.46	0.33	-2.49
Ag147-IH	IH	147	2.93	0.06	94.47	34.20	1.48	1.23	0.32	-3.62

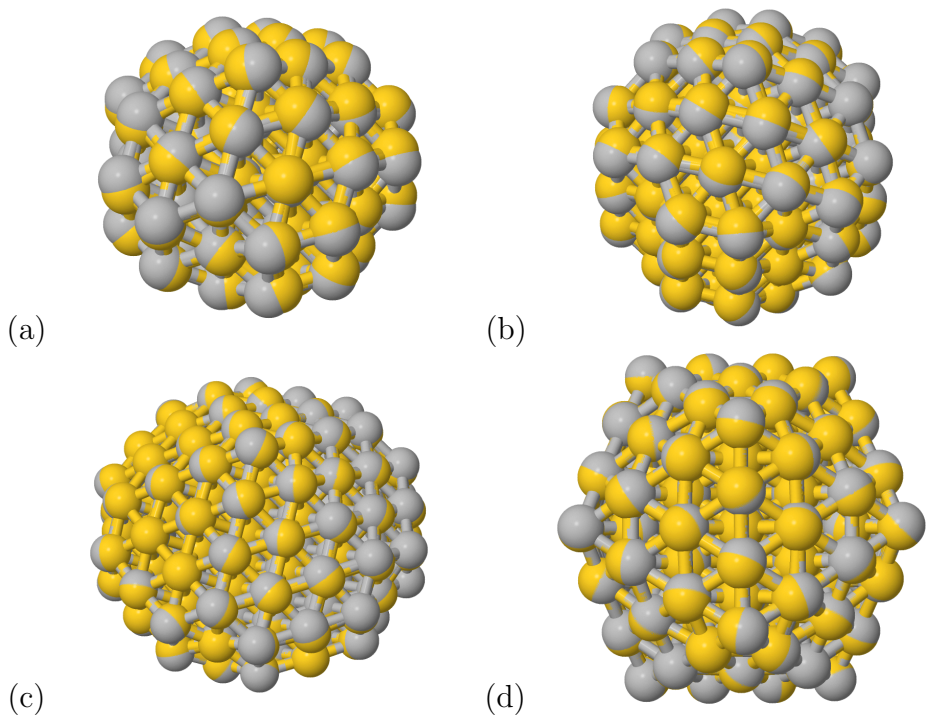

Figure 1: Geometry similarity of sample Ag nanoparticles (a) Ag75-DH, (b) Ag101-DH, (c) Ag146-DH and (d) Ag147-IH from DFTB (Yellow) and DFT (Grey) computation.

Thermodynamically Limited Boltzmann Distribution

Table 3: Boltzmann distribution, for samples that are thermodynamically limited: Shapes, with the probability distributed over all sizes.

	Expectation Values (eV)				Quality Factors (relative)			
	E_{Fermi}	IP	EA	E_{gap}	E_{Fermi}	IP	EA	E_{gap}
Tetrahedron	-3.82	4.10	3.51	0.59	1275.6%	139.1%	43.9%	-30.3%
Octahedron	-3.91	4.24	3.59	0.65	313.3%	294.3%	94.7%	2.7%
Truncated octahedron	-3.95	4.29	3.61	0.67	512.5%	274.5%	136.3%	12.8%
Cuboctahedron	-3.97	4.35	3.59	0.75	193.1%	414.5%	57.2%	12.7%
Truncated cube	-3.85	4.29	3.41	0.89	155.2%	144.6%	97.7%	72.9%
Truncated rhombic dodecahedron	-3.76	4.07	3.44	0.63	1328.3%	222.7%	180.8%	10.0%
Rhombic dodecahedron	-3.71	4.05	3.37	0.68	218.6%	168.8%	99.0%	16.7%
Rhombi-truncated octahedron	-3.78	4.14	3.42	0.72	50.1%	81.5%	12.2%	-3.1%
Modified truncated octahedron	-3.83	4.16	3.50	0.66	96.1%	72.0%	72.1%	10.5%
Small rhombicuboctahedron	-3.81	4.17	3.45	0.71	115.9%	103.9%	58.6%	8.9%
Great rhombicuboctahedron	-3.84	4.23	3.48	0.74	284.1%	37.8%	136.4%	6.2%
Tetrakis hexahedron	-3.77	4.10	3.43	0.67	684.2%	186.0%	188.4%	16.4%
Trapezohedron	-3.79	4.13	3.46	0.67	339.0%	267.6%	133.2%	28.1%
Triakis octahedron	-3.79	4.11	3.46	0.65	255.2%	234.5%	103.7%	16.0%
Hexakis octahedron	-3.81	4.15	3.47	0.69	301.9%	170.0%	43.4%	-23.7%
Decahedron *	-3.97	4.30	3.63	0.67	162.3%	118.1%	88.3%	1.4%
Icosahedron	-4.05	4.38	3.72	0.66	681.9%	239.5%	122.8%	-5.0%
All	-3.92	4.25	3.58	0.67	45	47	37	10

Table 4: Boltzmann distribution, for decahedra samples that are thermodynamically limited: Structure-constrained samples, with the probability distributed over all sizes.

	Expectation Values (eV)				Quality Factors (relative)			
	E_{Fermi}	IP	EA	E_{gap}	E_{Fermi}	IP	EA	E_{gap}
Simple Decahedron	-3.84	4.16	3.53	0.63	313.5%	636.3%	86.6%	6.8%
Ino Decahedron	-4.01	4.35	3.67	0.69	284.3%	168.4%	117.3%	10.7%
Marks Decahedron	-3.96	4.29	3.63	0.66	310.4%	210.6%	108.0%	8.4%

Table 5: Boltzmann distribution, for samples that are thermodynamically limited: Facet/Polyhedra-constrained-constrained samples, with the probability distributed over all sizes.

	Expectation Values (eV)				Quality Factors (relative)			
	E_{Fermi}	IP	EA	E_{gap}	E_{Fermi}	IP	EA	E_{gap}
Single Crystal	-3.83	4.16	3.49	0.67	11.0%	7.7%	8.3%	-1.6%
Twinned Crystal	-3.97	4.30	3.64	0.67	142.3%	105.9%	79.1%	1.0%
Simple	-3.88	4.23	3.53	0.70	-6.4%	-4.8%	-12.7%	-16.8%
Complex	-3.79	4.14	3.44	0.70	95.5%	57.0%	53.2%	-3.3%

Table 6: Boltzmann distribution, for samples that are thermodynamically limited: Index-constrained samples, with the probability distributed over all sizes.

	Expectation Values (eV)				Quality Factors (relative)			
	E_{Fermi}	IP	EA	E_{gap}	E_{Fermi}	IP	EA	E_{gap}
$n < 4$	-3.95	4.28	3.63	0.65	151.8%	120.5%	84.8%	4.2%
$n \geq 4$	-3.98	4.31	3.64	0.68	222.2%	154.6%	92.7%	2.0%
$p < 4$	-3.98	4.31	3.64	0.67	134.7%	87.3%	77.1%	-5.8%
$p \geq 4$	-3.95	4.28	3.62	0.66	375.9%	264.1%	120.2%	11.6%

Size-dependent Normal Distribution

Table 7: Normal distribution, for samples that are kinetically limited: Shapes, with the probability distributed over all sizes.

	Expectation Values (eV)				Quality Factors (relative)			
	E_{Fermi}	IP	EA	E_{gap}	E_{Fermi}	IP	EA	E_{gap}
Tetrahedron	-3.77	4.25	3.29	0.96	120.4%	-14.8%	-5.5%	-19.1%
Octahedron	-3.85	4.33	3.37	0.96	82.0%	30.0%	-9.0%	-13.0%
Truncated octahedron	-3.91	4.37	3.45	0.92	89.4%	20.3%	-14.9%	-25.3%
Cuboctahedron	-3.93	4.40	3.47	0.93	242.7%	43.5%	42.4%	12.9%
Truncated cube	-3.77	4.45	3.12	1.33	40.6%	2.5%	-39.4%	-11.7%
Truncated rhombic dodecahedron	-3.76	4.23	3.29	0.95	182.4%	-18.5%	38.4%	-10.1%
Rhombic dodecahedron	-3.69	4.11	3.27	0.84	237.7%	44.1%	63.9%	19.8%
Rhombi-truncated octahedron	-3.70	4.23	3.17	1.06	97.1%	-4.7%	-5.0%	-6.6%
Modified truncated octahedron	-3.82	4.23	3.41	0.82	173.9%	61.8%	83.3%	33.1%
Small rhombicuboctahedron	-3.78	4.22	3.34	0.88	115.7%	35.0%	101.9%	49.7%
Great rhombicuboctahedron	-3.82	4.26	3.40	0.86	191.7%	49.4%	57.2%	27.3%
Tetrakis hexahedron	-3.76	4.19	3.34	0.85	381.5%	39.3%	106.6%	29.5%
Trapezohedron	-3.78	4.18	3.37	0.82	284.6%	38.4%	58.0%	7.5%
Triakis octahedron	-3.72	4.19	3.26	0.93	54.7%	43.3%	-15.6%	-14.7%
Hexakis octahedron	-3.77	4.25	3.28	0.97	162.2%	43.2%	41.1%	25.7%
Decahedron *	-3.94	4.35	3.53	0.82	89.7%	52.4%	39.3%	10.3%
Icosahedron	-3.99	4.65	3.37	1.28	15.2%	-62.4%	-43.4%	-48.5%
All	-3.86	4.29	3.42	0.87	36	34	19	4

Table 8: Normal distribution, for decahedra samples that are kinetically limited: Structure-constrained samples, with the probability distributed over all sizes.

	Expectation Values (eV)				Quality Factors (relative)			
	E_{Fermi}	IP	EA	E_{gap}	E_{Fermi}	IP	EA	E_{gap}
Simple Decahedron	-3.75	4.33	3.18	1.15	44.4%	-47.5%	-47.5%	-45.9%
Ino Decahedron	-3.98	4.44	3.52	0.92	104.4%	0.8%	3.5%	-16.7%
Marks Decahedron	-3.94	4.33	3.55	0.78	232.3%	144.3%	89.8%	40.5%

Table 9: Normal distribution, for samples that are kinetically limited: Facet/Polyhedra-constrained-constrained samples, with the probability distributed over all sizes.

	Expectation Values (eV)				Quality Factors (relative)			
	E_{Fermi}	IP	EA	E_{gap}	E_{Fermi}	IP	EA	E_{gap}
Single Crystal	-3.78	4.24	3.32	0.92	34.0%	3.6%	10.7%	1.8%
Twinned Crystal	-3.94	4.36	3.53	0.83	80.1%	37.5%	30.3%	2.7%
Simple	-3.88	4.23	3.53	0.70	15.4%	31.9%	65.9%	104.5%
Complex	-3.79	4.14	3.44	0.70	141.0%	117.5%	191.1%	137.7%

Table 10: Normal distribution, for samples that are kinetically limited: Index-constrained samples, with the probability distributed over all sizes.

	Expectation Values (eV)				Quality Factors (relative)			
	E_{Fermi}	IP	EA	E_{gap}	E_{Fermi}	IP	EA	E_{gap}
$n < 4$	-3.91	4.35	3.47	0.88	40.4%	2.6%	-10.1%	-23.3%
$n \geq 4$	-3.96	4.35	3.58	0.77	214.5%	135.1%	141.4%	74.0%
$p < 4$	-3.94	4.38	3.51	0.87	75.8%	75.2%	66.1%	56.7%
$p \geq 4$	-3.94	4.30	3.58	0.73	377.5%	334.7%	228.7%	139.9%

References

(1) Perdew, J. P.; Burke, K.; Ernzerhof, M. Generalized Gradient Approximation Made Simple. *Phys. Rev. Lett.* **1996**, *77*, 3865–3868

(2) Blöchl, P. E. Projector Augmented-wave Method. *Phys. Rev. B* **1994**, *50*, 17953–17979.

(3) Kresse, G.; Joubert, D. From Ultrasoft Pseudopotentials to the Projector Augmented-Wave Method. *Phys. Rev. B*, **1999**, *59* 1758–1775

(4) Kresse, G.; Hafner, J. *Ab initio* Molecular Dynamics for Liquid Metals. *Phys. Rev. B* **1993**, *47*, RC558–561

(5) Kresse, G.; Hafner, J. Efficient Iterative Schemes for *Ab initio* Total-Energy Calculations Using a Plane-wave Basis set. *Phys. Rev. B* **1996**, *54*, 11169–11186

(6) Kresse, G.; Furthmüller, J. Efficiency of *Ab initio* Total Energy Calculations for Metals and Semiconductors Using a Plane-wave Basis Set. *Comp. Mat. Sci.*, **1996**, *6* 15–50

(7) Perdew, J. P.; Zunger, A. Self-interaction Correction to Density Functional Approximations for Many-Electron Systems. *Phys. Rev. B*, **1981**, *23* 5048–5079